Atomistic simulation of defect-dislocation interactions in concentrated solid-solution alloys

Shijun Zhao, Yuri Osetsky, and Yanwen Zhang

Phys. Rev. Materials **3**, 103602 — Published 8 October 2019

DOI: 10.1103/PhysRevMaterials.3.103602

Atomistic Simulation of Defect–Dislocation Interactions in Concentrated Solid–Solution Alloys

Shijun Zhao,[1,2,*] Yuri Osetsky,[2,†] and Yanwen Zhang[2,3]

[1] *Department of Mechanical Engineering, City University of Hong Kong, Hong Kong, China*
[2] *Materials Science and Technology Division, Oak Ridge National Laboratory, Oak Ridge, Tennessee 37831, USA*
[3] *Department of Materials Science and Engineering, University of Tennessee, Knoxville, Tennessee 37996, USA*

The interaction between point defects and dislocations plays a crucial role in governing material properties and microstructural evolutions under external stimuli, such as mechanical deformation and irradiation. Here we present an atomistic study of the interactions between point defects and dislocations in concentrated solid–solution alloys (CSAs). Using molecular statics and kinetic Monte Carlo methods, we demonstrate that the strain energy and stress field distribution induced by a dislocation in CSAs are highly inhomogeneous along the dislocation line, which leads to heterogeneity of defect–dislocation interactions. Specifically, the interactions are spatially different and screened by the random arrangement of different elemental species. Such localization of defect–dislocation interaction indicates that the 'dislocation–bias' mechanism that is a driving force for radiation–induced void swelling, can be suppressed in concentrated alloys.

I. INTRODUCTION

Interactions between point defects and dislocations have a significant influence on the mechanical properties and performance of materials under irradiation environment. On one hand, point defects may act as obstacles to impede dislocation movement[1], thus leading to materials strengthening. On the other hand, the stress field produced by dislocations alters the migration energy landscape of nearby point defect and may change defect diffusion mechanisms. It is generally accepted that edge dislocations are strong defect sinks that can absorb point defects, especially interstitials. This preferential absorption leads to a 'dislocation bias', which is the reason for void swelling in materials under irradiation[2–4]. Therefore, the understanding of defect–dislocation interaction is of pivotal importance to tailor the mechanical and irradiation properties of materials.

The continuum elasticity theory is an effective tool for describing defect–dislocation interactions in homogeneous materials, since the stress field beyond the dislocation core is independent of the core structure. However, in heterogeneous materials, the stress field depends on the compositions of both the core and the surroundings. Previous studies have shown that in recent developed concentrated solid–solution alloys (CSAs), including high–entropy alloys (HEAs)[5–7], the dislocation line exhibits significant fluctuations that are induced by the atomic–level heterogeneity[8,9]. In fact, it has been demonstrated that the excellent mechanical properties[10,11] and irradiation resistance[12–15] found in HEAs are closely related to this unique dislocation property due to the chemically–disordered structures. Indeed, experiments reveal that the dissociation distance of perfect dislocations shows a large variability in HEAs[16], and simulations indicate that this local–environment–dependent variation along the dislocation line provides the necessary strengthening mechanism responsible for their unusual mechanical properties[17–19]. The fluctuations also help to suppress defect cluster growth and enhance irradiation tolerance of HEAs by slowing down the long-range dislocation movement under ion irradiation[8,20]. In HEAs, the heterogeneity related to structural disorder leads to a heterogeneous distribution of stress field surrounding the dislocations, and the dislocation core effects should be considered. Such a heterogeneous stress field would have a significant influence on the defect–dislocation interactions.

The chemical disorder in HEAs not only induces heterogeneity at the atomic level, but also greatly changes the way that defects interact with each other at the electronic level. Notably, electron scattering in HEAs is enhanced significantly by the extreme degree of chemical disorder that limits the electron mean free path[12]. The perturbations induced by defects can be rapidly screened out by this disorder scattering, and the ability of defects to convey 'information' over long distances is greatly reduced relative to that in pure metals and dilute alloys. As a result, the interactions among different defects are predominantly dependent on the local environment around them. Characterizing such local interaction would need an atomistic description that is able to give precise atomic structures. The knowledge from atomistic simulations is also a necessary step for establishing and validate continuum models, especially the knowledge of interaction details in the dislocation core region.

In this study, we present results of an atomistic simulation of vacancy–dislocation interactions in concentrated alloys. Vacancy defects are chosen because of their well-defined jumps in the lattice (jumps between nearest neighboring sites), which is one of the most important considerations in Monte Carlo simulations. For simplicity, the equiatomic NiFe alloy is studied, and the results are compared with those in pure Ni. We first compare the strain energy and stress field distribution surrounding a 1/2[110] edge dislocation in pure Ni and NiFe, and show that the distributions are highly heterogeneous in

NiFe due to the chemical disorder. The interaction between a vacancy and the dislocation is then studied by the kinetic Monte Carlo (kMC) method with on-the-fly estimated migration barriers. We demonstrate that the vacancy can be easily trapped in local regions far from the dislocation in NiFe in most cases, instead of direct absorption observed in pure Ni. These results indicate that the defect–dislocation interaction is relatively weak in concentrated NiFe alloys.

II. METHOD

Molecular static simulations were performed using the large–scale atomic/molecular massively parallel simulator (LAMMPS)[21]. The interatomic interactions were described using the embedded–atom method (EAM) parameterized by Bonny et al.[22]. This potential has been proved to give consistent defect properties with density functional theory (DFT) results[23]. A 1/2[110] edge dislocation is created by joining together two half crystals, in which the upper half crystal had one more {110} lattice plane than the lower half, as described in previous studies[24]. After relaxation, a dissociated edge dislocation is produced; the dissociation distance depends on the stacking fault energy (SFE)[1]. The x, y and z directions of the simulation cell were oriented in the [110], $[\bar{1}11]$ and $[1\bar{1}2]$ crystalline directions, respectively. An illustration of the simulation setup can be found in our previous work[8]. Periodic boundary conditions were employed along the x and z directions, whereas free boundary condition was used in the y direction. The imposed periodic boundary condition in the x direction can induce stress inside the supercell, so the dimension in this direction should be large enough to accommodate the dislocation. We have tested different length in this direction from $100|b|$ to $500|b|$ (b is the Burgers vector) to ensure the results are not significantly influenced.

The strain energy of an edge dislocation stored in a cylinder at radius r with its axis along the dislocation line is calculated by:

$$E_s(r) = \frac{1}{N}\sum_i(\varepsilon_i^d - \varepsilon_i^p), \quad (1)$$

where ε_i^d and ε_i^p are the energies of atom i in the supercells with and without dislocations, respectively. The summation is over all N atoms that are inside the cylinder. The strain energy, therefore, includes contributions from the dislocation core. The stress field around the dislocation is calculated after energy minimization.

In this study, the defect–dislocation was investigated by simulating the interactions between a vacancy and an 1/2[110] edge dislocation. The simulation was carried out using a modified on-the-fly lattice kMC model with LAMMPS as the force calculator. The length of the simulation box was $200|b|$ along the x direction, and the size of the box was around 50050043 Å^3. After the dislocation was introduced in the center of the box, a single vacancy was created at a distance of 20 Å with respect to the center of the dislocation core to simulate their interactions. Only the first-nearest-neighbor jumps were considered according to local energy barriers that were calculated by directly optimizing the saddle configurations around the vacancy[25]. In all kMC simulations, an attempt frequency of 10^{13} Hz[26] and a temperature of 500 K were used. For each case, 5000 kMC steps (which is also the number of vacancy jumps) were simulated, unless the vacancy was absorbed by the dislocation earlier.

III. RESULT

A. Strain energy and strain field

We first compare the distribution of strain energy and stress field around a 1/2[110] edge dislocation in Ni and NiFe, as shown in Fig. 1. These results are obtained in a supercell with a length of $200|b|$ along the x direction. The dislocation is divided into small segments along the dislocation line with a separation of 30 Å, and the strain energies around 7 different dislocation segments are plotted. It can be seen that E_s in pure Ni around the 7 dislocation segments overlaps completely, an indication of the uniform distribution of strain energy along the dislocation line. However, in concentrated NiFe, the strain energy varies significantly around different dislocation segments, which is a result of the chemical disorder.

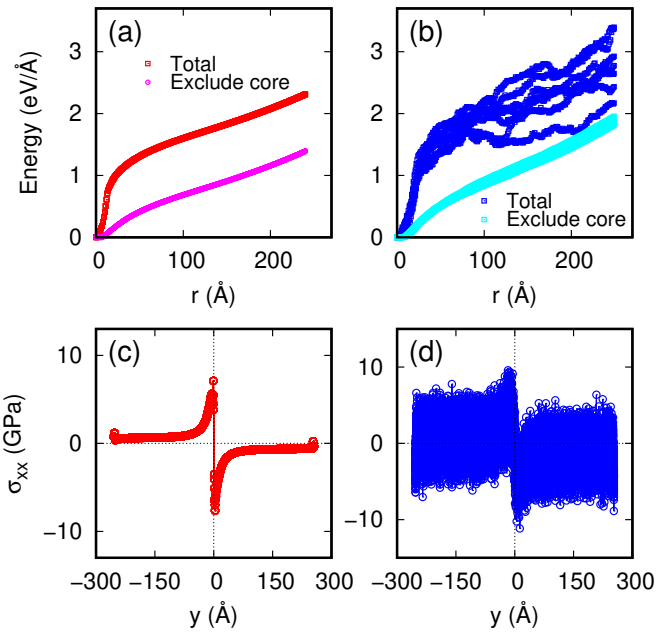

FIG. 1. Strain energy (the upper row) and stress field distribution (the lower row) in pure Ni ((a) and (c)) and concentrated NiFe ((b) and (d). For strain energy, the contributions included or excluded the atoms in the dislocation core are denoted.

The strain energy as calculated by Eq. 1 includes contributions from both the dislocation core and the elastic part outside the core: $E_s = E_{core} + E_{elastic}$. According to elasticity theory, the elastic part increases logarithmically with the cylinder radius r: $E_s = \frac{Gb^2}{4\pi(1-\mu)} ln(\frac{r}{r_0})$, where G is the shear modulus, b is the length of the Burgers vector, μ is the Poissons ratio, and r_0 is the radius of the dislocation core. In order to distinguish the two contributions in E_s, we have calculated E_s by including and excluding the atoms in the dislocation core. The cutoff distance of interatomic interactions in the used potential, i.e. 5.6 Å[22], is chosen as a criterion to exclude the dislocation core atoms. Therefore, only those atoms with $|y - y_0| > 5.6$ are included to calculate $E_{elastic}$, where y_0 is the y coordinates of the dislocation core center. After excluding the core contribution, the obtained $E_{elastic}$ shown in Fig.1(a and b) increases logarithmically with r for both Ni and NiFe, consistent with the prediction of elasticity theory. Thus the fluctuations in the total strain energy of NiFe originate from the dislocation core. Indeed, as revealed in previous studies, the dislocation core structures in concentrated alloys exhibit significant fluctuations due to the fluctuation of local SFEs[8].

The calculated stress field distribution around the dislocation in NiFe also shows significant fluctuations along the dislocation line, in contrast to the uniform distribution observed in pure Ni. The amplitude of stress fluctuations at different dislocation segments is as large as 15 GPa. The fluctuations in both strain energy and stress field distributions suggest that the interactions between the dislocation with surrounding defects (solutes or impurities) are highly heterogeneous. Therefore, the interaction between a defect and dislocation in NiFe is expected to be localized since every defect experiences unique local stress around the dislocation and the differences in stress at different regions can be remarkably high.

B. Vacancy–Dislocation interaction

The interaction between a 1/2[110] dislocation and a vacancy is simulated by placing the vacancy near the dislocation. Since previous studies have revealed that the stress surrounding an edge dislocation along the $x = y$ direction (45° to the dislocation slip plane) is the highest[24], we choose to put a vacancy along this direction. The possible vacancy sites are illustrated in Fig.2(a). In this study, the separation distance between the vacancy and the dislocation center is set to be 20 Å, which is large enough to prevent direct absorption of the vacancy by the dislocation and, at the same time, small enough to ensure the vacancy have interactions with the dislocation. The interaction between the introduced vacancy and the edge dislocation is then studied through the kMC procedure mentioned above. In our simulation, the dislocation core is minimized through both conjugate gradient and damped dynamics methods, which ensure the energy minimum is achieved. During the on-the-fly kMC, the dislocation-vacancy system is relaxed at each step to calculate the total energy and the migration barrier. We have checked that the dislocation core structure is stable against the vacancy diffusion and the vacancy absorption.

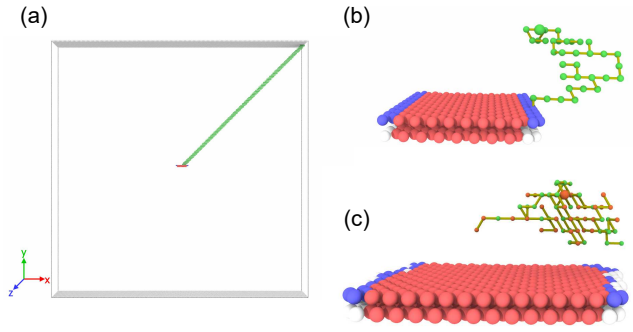

FIG. 2. Atomic configurations used in the simulations. (a) Illustration of the simulation setup to study the interaction between a vacancy and an edge dislocation. The dislocation is located at the center of the simulation box. The green spheres along the $x = y$ direction denote possible vacancy positions; (b) A trajectory of the vacancy that is absorbed by the dislocation in pure Ni, and (c) A trajectory of the vacancy that cannot be absorbed by the dislocation in NiFe within 5000 steps. The dislocation core atoms are shown by their structure types different from perfect *fcc*.

In a point defect–dislocation system, the defect can be absorbed by the dislocation due to their attractive interactions[27]. This is also the origin of 'dislocation bias' which states that point defects will aggregate preferentially into dislocations since they act as defect sinks. In pure Ni, our results indeed show that the vacancy is always absorbed by the dislocation during 10 different kMC simulations. A typical trajectory of the vacancy is shown in Fig. 2(b). Nevertheless, in NiFe, the vacancy just migrates in the system most of the time, without experiencing the interaction from the dislocation. As can be seen from the trajectory demonstrated in Fig. 2(c), the vacancy migrates around the dislocation but is not absorbed as observed in pure Ni. To further show this difference, we have analyzed the trajectories of the vacancy, and the results are summarized in Fig.3.

Fig. 3 reveals the differences in interaction mechanism between a vacancy and an edge dislocation in pure Ni and concentrated NiFe. In pure Ni, the absorption efficiency of the vacancy by the dislocation is high, as it makes a small number of jumps, ~200, before the absorption. On the contrary, in NiFe, in the majority of simulations (6 of 10), the vacancy is not absorbed by the dislocation, even after 5000 kMC steps. The calculated atomic squared displacement (ASD) of the vacancy indicates that the vacancy just jumping around a local region between the original location and the dislocation, since the ASD is almost independent of kMC steps after initial movement. This effect is attributed to the trapping of the vacancy by the local environment in chemically–disordered NiFe.

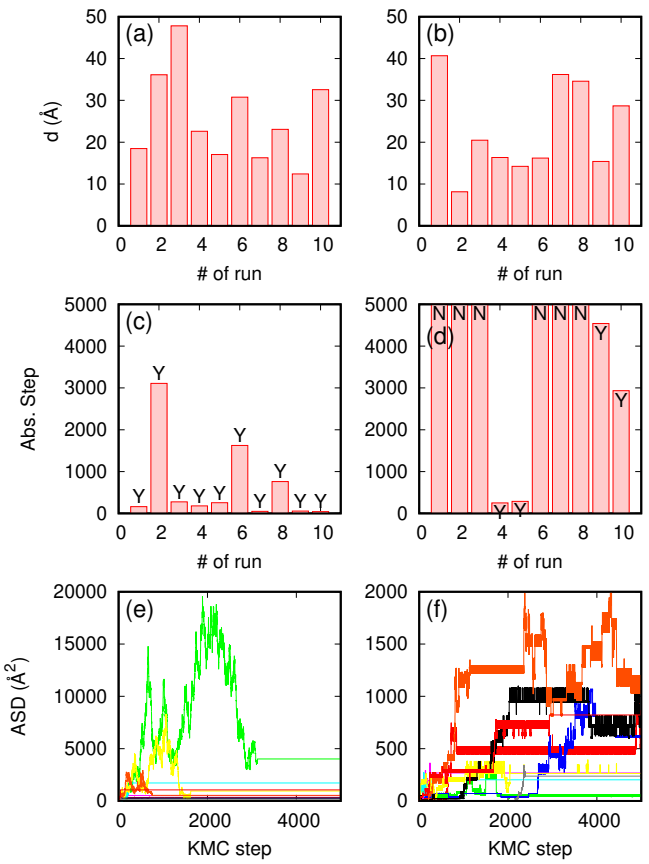

FIG. 3. Interaction between a vacancy with an edge dislocation in Ni (left column) and NiFe (right column) as simulated in 10 different kMC simulations. (a) and (b) show the travel distance of the vacancy up to 5000 kMC steps; (c) and (d) show the kMC steps before the vacancy is absorbed by the dislocation. Whether the vacancy is absorbed or not is indicated by 'Y' and 'N'; (e) and (f) display the atomic squared displacement of the vacancy.

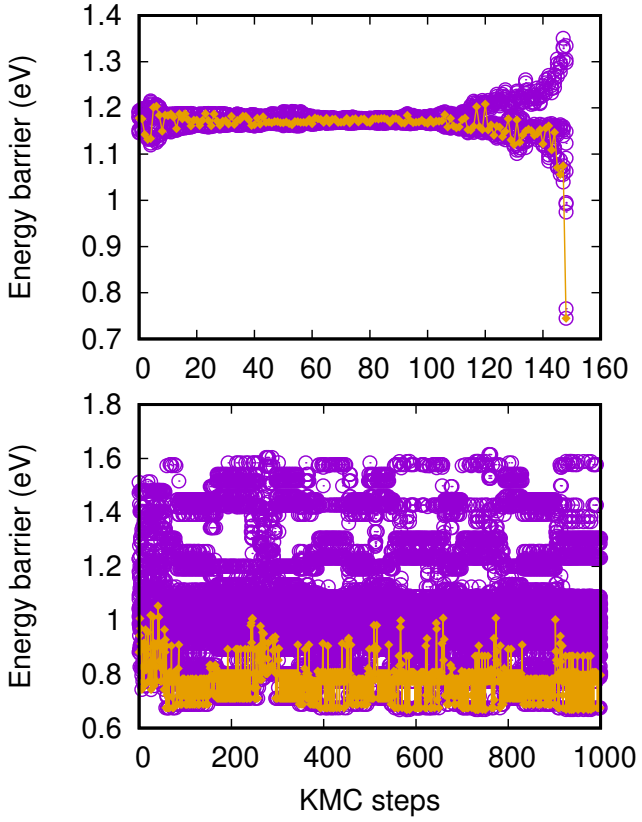

FIG. 4. Calculated 12 energy barriers for vacancy migration at each position around an edge dislocation in pure Ni and NiFe. The executed barriers during kMC simulations are denoted by orange lines. In (a), the vacancy is absorbed by the dislocation after 147 steps, whereas the vacancy cannot be absorbed in NiFe as illustrated in (b). For clarity, the barriers for the first 1000 steps are shown.

The random arrangement of elements induces a rough energy landscape for vacancy diffusion, which creates lots of defect traps that restrict the vacancy within local energy valleys and induce strong correlations in its jumps[13]. This trapping effect is larger than the attraction effect caused by the dislocation[26]. As a result, the vacancy just moves around local "traps" that screen the interactions with the dislocation.

The trapping effect can be further analyzed by the migration energy barriers of the vacancy. In pure Ni, the energy barrier is 1.17 eV based on the used empirical potential[23]. For each vacancy position, 12 barriers are calculated corresponding to the 12 possible nearest neighbor jumps. Among these 12 possibilities, the actual jump is chosen based on the Metropolis algorithm[28]. The energy barriers calculated and executed in pure Ni and NiFe are plotted in Fig. 4.

Fig. 4 shows that the vacancy migration barriers in pure Ni are not much influenced by the dislocation until the vacancy is near the dislocation core. The executed barriers (orange line and symbols) are distributed in a narrow range from 1.1 to 1.2 eV away from the dislocation core, while they become significantly lower near the dislocation core region. However, in the NiFe alloy, the energy barriers are widely distributed at different locations. The calculated distribution (blue line and symbols) ranges from 0.7 to 1.6 eV, which is similar to those in bulk NiFe calculated with accurate NEB method[23,29]. By looking into the executed barriers, we find that almost every vacancy jump proceeds through Fe sites. This observation is consistent with the chemically-biased diffusion in concentrated NiFe, as revealed in previous *ab initio* and classical MD simulations[23,26,29,30]. Specifically, vacancy migration through exchange with Fe sites exhibits low energy barriers. Therefore, the vacancy is more likely to be trapped when the surroundings of the vacancy are mostly composed of Ni atoms, since the vacancy prefers to migrate through Fe sites. In this case, the vacancy is trapped in this local region for a long time,

hardly experiencing the interaction from the dislocation. Therefore, the efficiency of defect absorption by dislocations in NiFe is greatly reduced.

IV. DISCUSSION

Because of the different migration barriers in pure Ni and NiFe as demonstrated in Fig.4, the timescale simulated in the on-the-fly kMC is different. Indeed, vacancy migration barriers are distributed widely in concentrated alloys[23,29,31], and in general, vacancy exchange with Fe atoms has lower barriers. During diffusion, vacancy jumps would follow the low-barrier trajectories as demonstrated in Fig.4(b). Due to the lower energy barriers in concentrated alloys, the effective simulation time in kMC is shorter than that in pure Ni. In pure Ni, the adsorption of vacancy is very quick after dozens of kMC steps, i.e. defect jumps, corresponding to a time span ~0.10.5 seconds. However, in alloys, the time span is around 0.010.08 seconds even after 5000 kMC steps. Inspection of the trajectory reveals that the vacancy just moves back and forth for more than 1500 steps, demonstrating strongly correlated diffusion with a low value of defect jump correlation factor. In these cases, the vacancy effectively gets trapped in the local configuration that is defined by a few low barriers for the vacancyFe exchange. For example, we observed a particular case when the lowest barrier for the vacancyFe exchange was ~0.78 eV while all others were >0.2 eV higher. As a result, a vacancy jumped forward and backward according to the low-energy exchange with the same Fe atom several thousand times without producing long-range diffusion. The diffusion drift force is defined by the gradient of the vacancydislocation elastic interaction energy. The interaction energy can approximate as $p\Delta\Omega$ where p is the local pressure and $\Delta\Omega$ is the vacancy dilatation volume roughly equal to the atomic volume. This energy is in the order of ~0.01 eV at 20 Åaway from the dislocation core. The energy difference for vacancy jumps in and out is even an order in magnitude lower. Thus the contribution from the drift force is quite low relative to the difference in jump barriers, 0.2 eV. The trap of vacancies is a result of the disordered state inherent in concentrated alloys. Another reason is the usage of a constant jump frequency in the estimation of time and probability for defect jumps, though this is a common problem in kMC modeling approach. These two factors lead to different time scale simulated in pure metal and concentrated alloys.

We have shown the heterogeneous nature of defect–dislocation interactions in concentrated alloys based on the kMC simulations. Although the average trend of elastic energy and stress field surrounding the dislocation in alloys is similar to that in pure Ni, Fig.1(d) demonstrates huge fluctuations in stress in the alloys compared to in pure metal, which strongly affect the defect diffusion process. In this case, the defect jumps proceed not under average conditions but under both local and the drift force of dislocation, as defined by the dislocation stress field. Existence of fluctuations is evidence that the process of defect–dislocation interactions cannot be considered as a simple drift diffusion under the influence of a conventional dislocation strain/stress field. Local fluctuations may exceed many times the dislocation-related stress/strain and thus affect defect diffusion towards the dislocation core. Indeed, the on-the-fly kMC modeling demonstrate this complexity of defect–dislocation interactions in the concentrated alloys. The results show that the interaction is weakened and the defect trajectory before it can be absorbed by a dislocation, is longer than that in pure metal. In addition, in concentrated alloys, the diffusion of defects becomes sluggish and chemically-biased[26,29]. These factors can also affect defect–dislocation interactions. In fact, these are additional effects which also work towards decreasing the "dislocation bias" because the sluggish effect is stronger for interstitial diffusion. The local stability of interstitial atoms fluctuates much stronger than that of vacancies. Therefore, the drift effects in diffusion, that are defined as the defect formation energy difference after defect jumps towards and away from a dislocation, are less effective for interstitial atoms. Consequently, in general, the efficiency of the dislocation to capture defects is weaker in CSAs. Due to the larger local fluctuations in the interstitial atom formation energies, their diffusion is less affected by the drift forces.

It should be noted that the overall vacancy diffusivity is higher in NiFe compared to in pure Ni, as demonstrated in previous studies[23,26,29]. Therefore, the characteristic capture time of a vacancy by the dislocation should be shorter in concentrated NiFe than in pure Ni. According to the published diffusivity data, the ratio of diffusivity D^*_{NiFe}/D^*_{Ni} becomes higher with decreasing temperature. The ratio at 500 K is around 10, an order of magnitude higher, which suggests that the capture time in NiFe should be one order lower than that in pure Ni. To further elucidate the influence of simulation time, we have continued the simulation in the alloy case, until the simulation time reaches the same order as that in pure Ni. The results show that vacancy absorption occurs in one case when we increase the simulation time to at least 0.1 s. Thus, the efficiency of vacancy absorption is slightly influenced by the simulation time. The results support that the vacancy is more difficult to be absorbed by the dislocation in concentrated NiFe, even within the same time scale.

The "dislocation bias" is one of the most important factors contributing to the swelling phenomena in metals and alloys. There are also other mechanisms proposed in the literature. For example, it is suggested that the large difference between elastic relaxation volumes of interstitials and vacancies could generate local volumetric expansion, which may also lead to swelling in systems with a high concentration of the interstitial-type defects[32]. However, dislocation loops, which is the

majority of interstitial clusters formed under irradiation, should be excluded from this consideration since they are usually treated as a dislocation line with the corresponding bias in interactions with vacancies and interstitials. Such dislocation loop bias would depend on the loop size. In this study, we focus on the conventional "dislocation bias" that is described as a driving force for swelling in most cases.

In the NiFe alloy, there are some vacancies can reach the dislocation core region and be absorbed, as shown in our kMC results. These events, due to the chemically-biased diffusion, will lead to Ni segregation around these dislocation segments by transporting Fe atoms out of the core. The resulting local enrichment of Ni around the dislocation region then may reduce further the flow of vacancies to these segments, thus the defect–dislocation interactions may become even weakened gradually.

V. CONCLUSION

Defect–dislocation interactions in concentrated NiFe alloys are simulated and the results are compared to those in pure Ni. Firstly, we show that the strain energy and stress field around an edge dislocation are highly heterogeneous at different dislocation segments in NiFe alloys, in contrast to homogeneous distributions in pure Ni. This variation in NiFe along the dislocation line is related to the fluctuations in the dissociation distance between the two partials, which is caused by local configurations due to chemical disorder. We further show that, since the vacancy prefers to migrate through Fe sites due to lower migration barriers, the vacancy can be trapped away from the dislocation core most of the time. As a result, the interaction between a vacancy and an edge dislocation is relatively weak in NiFe. Although only vacancy defects are considered, the heterogeneous interaction mechanisms reveal here should also be applicable for interstitials. Thus our results indicate the ability of dislocations to absorb point defects in concentrated NiFe is reduced compared to that in pure Ni. Thus the effect of 'dislocation bias' responsible for void swelling should be suppressed, which leads to enhanced irradiation resistance of concentrated alloys.

VI. ACKNOWLEDGMENTS

This work was supported as part of the Energy Dissipation to Defect Evolution (EDDE), an Energy Frontier Research Center (EFRC) funded by the U.S. Department of Energy, Office of Science, Basic Energy Sciences under contract number DE-AC05-00OR22725. Shijun Zhao is grateful for the financial support from City University of Hong Kong (No. 9610425), Research Grants Council of Hong Kong (No. 21200919), and National Natural Science Foundation of China (No. 11975193).

* shijzhao@cityu.edu.hk
† osetskiyyn@ornl.gov

[1] D. Hull and D. J. Bacon, *Introduction to dislocations* (Butterworth-Heinemann, MA, 2011).
[2] G. Greenwood, A. Foreman, and D. Rimmer, Journal of Nuclear Materials **1**, 305 (1959).
[3] R. Konings, *Comprehensive nuclear materials* (Elsevier, 2011).
[4] G. S. Was, *Fundamentals of radiation materials science: metals and alloys* (Springer Science & Business Media, 2007).
[5] D. Miracle and O. Senkov, Acta Materialia **122**, 448 (2017).
[6] J.-W. Yeh, S.-K. Chen, S.-J. Lin, J.-Y. Gan, T.-S. Chin, T.-T. Shun, C.-H. Tsau, and S.-Y. Chang, Advanced Engineering Materials **6**, 299 (2004).
[7] B. Cantor, I. Chang, P. Knight, and A. Vincent, Materials Science and Engineering: A **375**, 213 (2004).
[8] S. Zhao, Y. N. Osetsky, and Y. Zhang, Journal of Alloys and Compounds **701**, 1003 (2017).
[9] Y. N. Osetsky, G. M. Pharr, and J. R. Morris, Acta Materialia (2018).
[10] B. Gludovatz, A. Hohenwarter, D. Catoor, E. H. Chang, E. P. George, and R. O. Ritchie, Science (New York, N.Y.) **345**, 1153 (2014).
[11] B. Gludovatz, A. Hohenwarter, K. V. S. Thurston, H. Bei, Z. Wu, E. P. George, and R. O. Ritchie, Nature Communications **7**, 10602 (2016).
[12] Y. Zhang, G. M. Stocks, K. Jin, C. Lu, H. Bei, B. C. Sales, L. Wang, L. K. Béland, R. E. Stoller, G. D. Samolyuk, M. Caro, A. Caro, and W. J. Weber, Nat. Comm. **6**, 8736 (2015).
[13] Y. Zhang, S. Zhao, W. J. Weber, K. Nordlund, F. Granberg, F. Djurabekova, F. Granbergc, and F. Djurabekova, Current Opinion in Solid State and Materials Science **21**, 221 (2017).
[14] Y. Zhang, K. Jin, H. Xue, C. Lu, R. J. Olsen, L. K. Beland, M. W. Ullah, S. Zhao, H. Bei, D. S. Aidhy, G. D. Samolyuk, L. Wang, M. Caro, A. Caro, G. M. Stocks, B. C. Larson, I. M. Robertson, A. A. Correa, and W. J. Weber, Journal of Materials Research **31**, 2363 (2016).
[15] C. Lu, L. Niu, N. Chen, K. Jin, T. Yang, P. Xiu, Y. Zhang, F. Gao, H. Bei, S. Shi, M.-R. He, I. M. Robertson, W. J. Weber, and L. Wang, Nature Communications **7**, 13564 (2016).
[16] T. Smith, M. Hooshmand, B. Esser, F. Otto, D. McComb, E. George, M. Ghazisaeidi, and M. Mills, Acta Materialia **110**, 352 (2016).
[17] C. Varvenne, A. Luque, and W. A. Curtin, Acta Materialia **118**, 164 (2016).
[18] C. Varvenne, G. P. M. Leyson, M. Ghazisaeidi, and W. A. Curtin, Acta Materialia **124**, 660 (2017).
[19] Y. Zeng, X. Cai, and M. Koslowski, Acta Materialia **164**, 1 (2019).
[20] F. Granberg, K. Nordlund, M. W. Ullah, K. Jin, C. Lu, H. Bei, L. M. Wang, F. Djurabekova, W. J. Weber, and

Y. Zhang, Physical Review Letters **116**, 135504 (2016).
[21] S. Plimpton, J. Comput. Phys. **117**, 1 (1995).
[22] G. Bonny, D. Terentyev, R. C. Pasianot, S. Poncé, and A. Bakaev, Modell. Simul. Mater. Sci. Eng. **19**, 85008 (2011).
[23] S. Zhao, G. M. Stocks, and Y. Zhang, Phys. Chem. Chem. Phys. **18**, 24043 (2016).
[24] Y. N. Osetsky and D. J. Bacon, Modelling and Simulation in Materials Science and Engineering **11**, 427 (2003).
[25] S. Zhao, T. Egami, G. M. Stocks, and Y. Zhang, Physical Review Materials **2**, 013602 (2018).
[26] Y. N. Osetsky, L. K. Béland, A. V. Barashev, and Y. Zhang, Current Opinion in Solid State and Materials Science **22**, 65 (2018).
[27] L. Casillas-Trujillo, A. S. Ervin, L. Xu, A. Barashev, and H. Xu, Physical Review Materials **2**, 103604 (2018).
[28] A. F. Voter, in *Radiation Effects in Solids*, edited by K. E. Sickafus, E. A. Kotomin, and B. P. Uberuaga (Springer Netherlands, Dordrecht, 2007) pp. 1–23.
[29] Y. N. Osetsky, L. K. Béland, and R. E. Stoller, Acta Materialia **115**, 364 (2016).
[30] S. Zhao, Y. Osetsky, and Y. Zhang, Acta Materialia **128**, 391 (2017).
[31] S. Zhao, G. Velisa, H. Xue, H. Bei, W. J. Weber, and Y. Zhang, Acta Materialia **125**, 231 (2017).
[32] S. L. Dudarev, D. R. Mason, E. Tarleton, P.-W. Ma, and A. E. Sand, Nuclear Fusion **58**, 126002 (2018).